Macromolecules
COMMUNICATION TO THE EDITOR

DOI: 10.1021/ma102293z

Stabilization of 3D Network Morphologies in Thin Films via Chemical Modification of ABC Triblock Terpolymers

Alexandra Sperschneider,[†] Felix H. Schacher,[‡] Larisa Tsarkova,*[,§] Alexander Böker,*[,§,⊥] and Axel H. E. Müller[†]

[†]*Makromolekulare Chemie II, Universität Bayreuth, 95440 Bayreuth, Germany,* [‡]*Laboratory of Organic and Macromolecular Chemistry (IOMC), Friedrich-Schiller-Universität Jena, Humboldtstrasse 10, 07743 Jena, Germany,* [§]*DWI an der RWTH Aachen e.V., Pauwelsstrasse 8, 52056 Aachen, Germany, and* [⊥]*Lehrstuhl für Makromolekulare Materialien und Oberflächen, RWTH Aachen University, 52056 Aachen, Germany*

Received October 7, 2010
Revised Manuscript Received November 19, 2010

The increasing technological demand for structure minimization down to the nanoscale has urged scientists to look at both self- and guided-assembly of block co- and terpolymers in thin films. Current applications of block copolymer nanostructures range from nanolithography and electronics[1,2] to novel functional polymeric membranes with tailored properties.[3] The technological potential of BCs is based on their intrinsic rich and intriguing phase behavior in thin films[4] and on the possibilities to control both the dimensions and the functionality of the resulting microstructures.

An extreme challenge is to guide block copolymers toward the formation of interconnected 3-dimensional structures in thin films (i.e., under confinement) when the combined effect of the film interfaces and the commensurability of the finite film thickness with the characteristic structural dimension always break the symmetry of the bulk lattice. In most equilibrium cases, the confinement results in the alignment of the microdomains parallel to the film plane, with the structure having a planar 2D symmetry.[5] Relatively few investigations have focused on thin films of block copolymers that adopt network morphologies in the bulk (see recent review by Meuler et al.[6]). The most successful approach toward bicontinuous morphologies in thin films so far utilized blends of lamella-forming PS-*b*-PMMA diblock copolymers and respective homopolymers which were deposited on chemically patterned substrates.[7] This strategy led to the formation of complex bicontinuous structures at certain film thicknesses. More recently, 3D structures in relatively thick films from amphiphilic poly(styrene-*co*-acrylonitrile)-*b*-poly(ethylene oxide)-*b*-poly(styrene-*co*-acrylonitrile) triblock copolymers have been prepared via the solvent-induced transition from spherical to wormlike micelles.[8] The resulting material showed good mechanical properties which enabled the preparation of free-standing films. In relatively thick polystyrene-*b*-polyisoprene diblock copolymer films an epitaxial phase transition from a well-resolved double gyroid to a cylinder phase has been accessed with transmission electron microtomography.[9] Theoretical predictions on interconnected hybrid structures in thin films have been made by Lyakhova et al. using dynamic density functional theory (DDFT) simulations of a slit with highly asymmetric surfaces.[10]

*Corresponding authors. E-mail: tsarkova@dwi.rwth-aachen.de (L.T.); boeker@dwi.rwth-aachen.de (A.B.).

In this work we demonstrate the high efficiency of selective chemical modification to tune the microphase separation of polybutadiene-*block*-poly(2-vinylpyridine)-*block*-poly(*tert*-butyl methacrylate (BVT) terpolymers. We further achieve the stabilization of continuous complex mesostructures in films with a thickness of about two characteristic structural dimensions. Oxidative hydroboration of the PB block increases its polarity and its surface tension which induces drastic changes in both the interactions of the blocks with the confining surfaces and the enthalpic interactions between the different compartments of the terpolymer. Depending on the composition of the starting BVT terpolymer ($B_{53}V_{24}T_{23}^{85}$ or $B_{14}V_{18}T_{68}^{165}$, after modification denoted as HO-BVT^{85} and HO-BVT^{165}, respectively), we report on two different microphase-separated morphologies for the hydroborated derivatives: a spongelike porous structure and a bicontinuous cylindrical morphology. Note that subscripts refer to the volume fractions of the corresponding blocks and the superscript is the overall molecular weight in kg/mol.

The BVT block terpolymers studied here were synthesized via sequential living anionic polymerization as described earlier.[11] Selective hydroboration of the polybutadiene (PB) block has been done in accordance with refs 12 and 13. Thin films were prepared via spin-casting from 5 and 10 g/L solutions in chloroform onto polished silicon wafers (CrysTec) and annealed under a controlled vapor pressure of chloroform (80%) for 24−48 h followed by a fast quench with dry nitrogen. Under these well-controlled annealing conditions the polymer volume fraction in the film is well above 50%,[14] which implies that the swollen structure is within the intermediate segregation regime. The thin film morphology of the two BVT samples and their hydroborated derivatives has been investigated under identical preparation and processing conditions with TappingMode scanning force microscopy (SFM) (Dimension 3100 with NanoScope IV SPM controller, Vecco Instruments Inc.) and with scanning electron microscopy (SEM) (LEO 1530, Zeiss).

The phase behaviors of BVT^{85} and its hydroborated derivative, HO-BVT^{85}, are compared in Figure 1. A typical height SFM image of an equilibrated ∼105 nm thick BVT^{85} film (Figure 1a) displays a nanoscopically smooth, featureless surface with typical surface relief structures: round-shaped holes (dark color) which represent terraces with an absolute thickness of 67 ± 2 nm and with a corresponding step height between adjacent terraces of 38 ± 2 nm. The formation of terraces (regions with quantized film thickness) confirms a planar symmetry of the intrinsic microphase-separated structure. Such behavior could be attributed to a lamella phase which is aligned parallel to the film plane due to selective interactions of the PB block with the film surfaces. A close examination of the cross-sectional SEM image in Figure 1b further supports this observation.

Films from HO-BVT^{85} with a thickness in the range of 45−155 nm upon examination with SFM reveal macroscopically and microscopically smooth featureless surfaces with a glassy top layer (inset in Figure 1c).[15] Importantly, in contrast to the films from non-modified BVT, samples of HO-BVT^{85} did not exhibit any signs of terrace formation which is indicative of a true 3D morphology. During SEM measurements, the P*t*BMA top layer was removed through radiation damage revealing a meshlike matrix consisting of the two remaining

Published on Web 12/02/2010

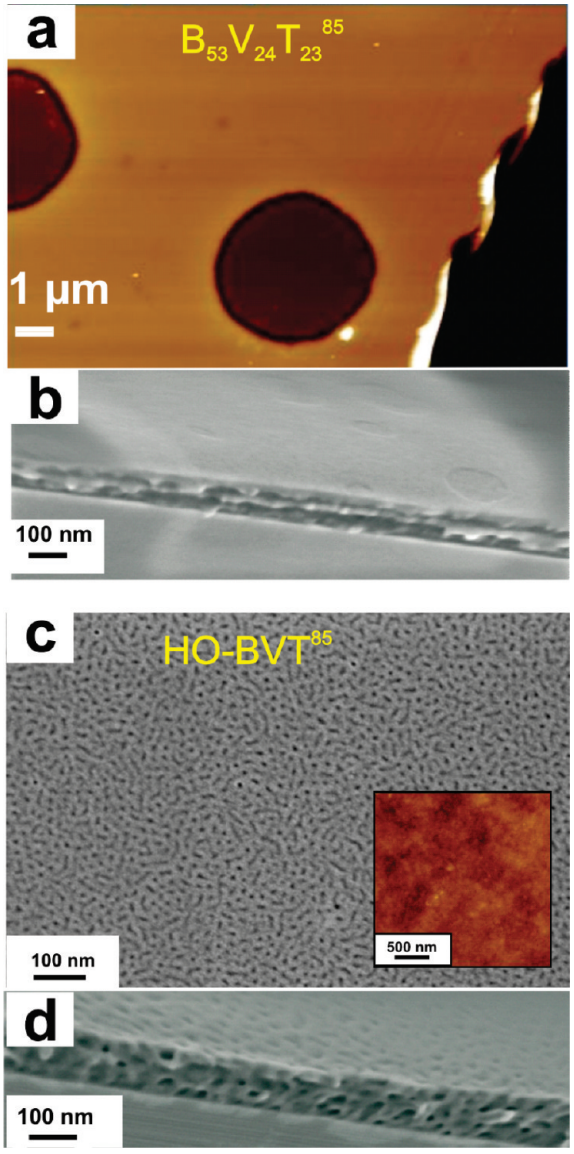

Figure 1. Microphase-separated structures in thin films of BVT^{85} (a, b) and its hydroborated derivative HO- BVT^{85} (c, d): SFM topography image (height scale 150 nm) (a), SEM image (c), and cross-sectional SEM images (b, d) of respective films in (a) and (c). Before imaging films have been equilibrated under chloroform vapor atmosphere for 24 h.

components, HO-PB and P2VP (Figure 1c). Cross-sectional SEM (Figure 1d) discloses that the P*t*BMA block can be successfully removed throughout the whole film thickness. The nanoporous spongelike structures displayed in Figure 1d represent a stable pattern which was detected over the whole studied film thickness.

In the case of BVT^{165}, where PB is the minority block, solvent-annealed films in a thickness range of 35−115 nm showed macroscopically smooth surfaces without any macroscopic topographic features: terraces or dewetting artifacts. Figure 2a displays a typical SFM topography image of a microphase-separated BVT^{165} film with the bright meshlike areas corresponding to the combined glassy P2VP and P*t*BMA components which cannot be distinguished in tapping mode. The dark cavities represent indentations (inset to Figure 2a) resulting from the segregation of the soft PB block to the free surface. The detailed identification of the microphase-separated pattern in BVT^{165} films has been reported earlier.[16,17] Depending on the film thickness, the structure has been assigned either to core−shell cylinders[16]

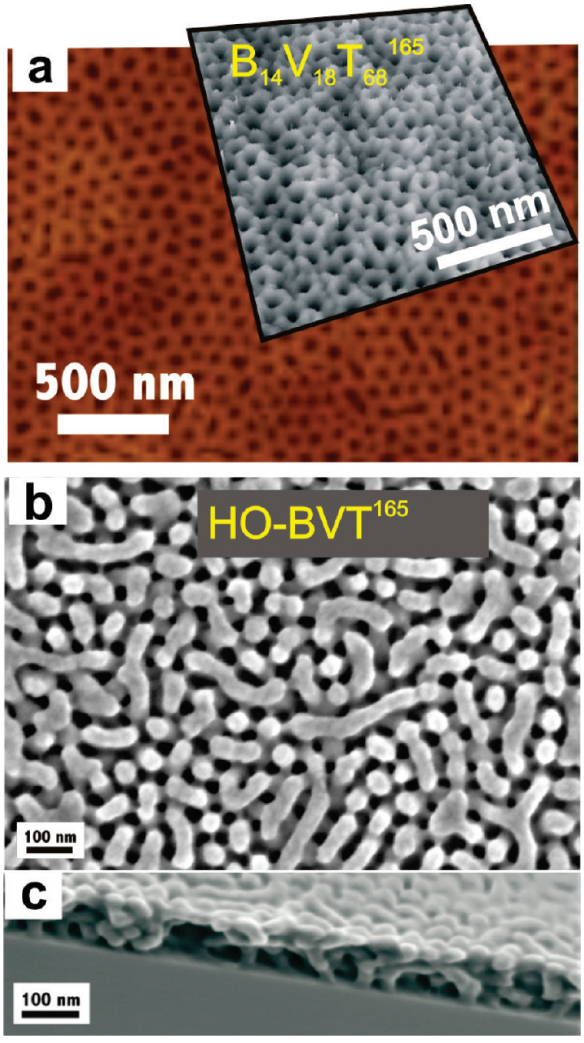

Figure 2. Microphase-separated structures in thin films of BVT^{165} (a) and its hydroborated derivative HO-BVT^{165} (b, c). SFM topography image (height scale 10 nm); inset: 3D SFM topography image (a), SEM image (b), and cross-sectional SEM images (c) of the film in (b). Before imaging films have been equilibrated under chloroform vapor atmosphere for 48 h.

or to standing three-component cylinders which are distorted under strong surface fields.[17]

The phase behavior in thin films of the hydroborated terpolymer HO-BVT^{165} is displayed in Figure 2b,c. Films with thicknesses in the range of 45−120 nm again were topographically smooth, and SFM imaging (not shown) detected a glassy wetting layer which prohibited the probing of underlying structures. SEM measurements revealed a hybrid structure which appeared after the destruction of the top P*t*BMA layer by the e-beam. The cross-sectional SEM in Figure 2c highlights a complex cylindrical structure where only two phases can be distinguished: the majority P*t*BMA matrix (which is removed during the SEM measurements) and the features with a cylindrical shape. We note that in contrast to the initial BVT^{165} terpolymer[16,17] no phase separation between HO-PB and P2VP blocks can be detected. Tentatively, we attribute this to hydrogen bonding occurring between HO-PB and P2VP. The combined volume fractions of both compartments would add to 32%, which is well in the stability regime of a cylindrical phase of an AB diblock copolymer in bulk.

The structure shows asymmetric wetting conditions and strong surface-field determined behavior: the segregation of the low-surface-energy P*t*BMA block to the free surface

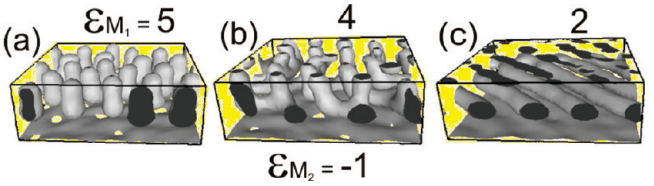

Figure 3. MesoDyn simulations of an ABA triblock copolymer in an asymmetric slit with effective parameters ε_{Mi} ($\varepsilon_M = \varepsilon_{AM} - \varepsilon_{BM}$) characterizing the strength of each surface field. Here the upper surface is selective for the A block ($\varepsilon_{M1} > 0$), and the lower surface is selective for the B block ($\varepsilon_{M2} < 0$). Reproduced with permission from ref 5. Copyright 2004 American Institute of Physics.

drives the cylinders to be oriented in-plane, while both enthalpic and entropic factors favor the cylinder ends at the silicon substrate. Therefore, the orientation of the cylindrical domains can be tuned by each surface interaction.

Further, the interpretation of the structure has been facilitated by the comparison with the theoretical computational study of an ABA triblock copolymer (which also reflects the behavior of a similar AB diblock copolymer[18]) in an asymmetric film (Figure 3) where the interactions between the components and the top (ε_{M1}) and bottom (ε_{M2}) interface have been varied in a wide range.[10] Under asymmetric boundary conditions, the authors detected a hybrid structure (Figure 3b) which was attributed to the coexistence of different surface reconstructions close to the interfaces when the cylinders interconnect in order to combine the perpendicular and parallel structures. Such phase behavior is modulated by the film thickness via interference and confinement effects in a very complicated manner. The similarity of the simulations using the dynamic density functional theory (Figure 3b) and of the experimental results (Figure 2c) strongly indicates that the microphase-separated pattern of HO-BVT^{165} is governed by the surface fields rather than it represents a nonequilibrium morphology under low chain mobility conditions.

In conclusion, the thin film phase behavior of two BVT samples and their hydroborated derivatives has been studied under identical preparation and processing conditions. This allows us to assign the observed morphological differences merely to the chemical modification and the resulting changes in polymer−polymer and polymer−interfaces interaction parameters. In the original BVT samples, the large differences in surface tension of the PB block and the two glassy components strongly affect the microphase separation in thin films, either by "top-to bottom" directing a structure with a planar symmetry (BVT^{85}) or by distortion of the unit cells due to asymmetric interfacial interactions (BVT^{165}). Oxidative hydroboration resulted in balancing the interactions of the terpolymer components with both confining surfaces. This resulted in the stabilization of complex network morphologies in thin films.

With this approach, we fabricated two types of nanoporous films. Because of the high molecular weight of the studied BVT triblock terpolymers, their films proved to be stable toward dewetting under controlled solvent annealing treatment. The presence of a third compartment facilitates the formation of nanoscale pores or continuous network mesostructures. Because of thickness independence and high homogeneity of the pattern over macroscopically large areas, both discovered morphologies are highly promising for, e.g., composite membrane technologies.

Acknowledgment. This project was supported by Volkswagen-Stiftung in the framework of the project Complex Materials. The authors thank G. J. A. Sevink and A. V. Zvelindovsky for fruitful discussions.

References and Notes

(1) Hamley, I. W. *Prog. Polym. Sci.* **2009**, *34* (11), 1161–1210.
(2) Li, M.; Coenjarts, C. A.; Ober, C. K. *Adv. Polym. Sci.* **2005**, *190* (Block Copolymers II), 183−226.
(3) Jackson, E. A.; Hillmyer, M. A. *ACS Nano* **2010**, *4* (7), 3548–3553.
(4) Krausch, G.; Magerle, R. *Adv. Mater.* **2002**, *14* (21), 1579.
(5) Tsarkova, L.; Sevink, G. J. A.; Krausch, G. *Adv. Polym. Sci.* **2010**, *227* (Complex Macromolecular Systems I), 33−73.
(6) Meuler, A. J.; Hillmyer, M. A.; Bates, F. S. *Macromolecules* **2009**, *42* (19), 7221–7250.
(7) Daoulas, K. C.; Muller, M.; Stoykovich, M. P.; Park, S.-M.; Papakonstantopoulos, Y. J.; de Pablo, J. J.; Nealey, P. F.; Solak, H. H. *Phys. Rev. Lett.* **2006**, *96* (3), 036104/1−4.
(8) Quemener, D.; Bonniol, G.; Phan, T. N. T.; Gigmes, D.; Bertin, D.; Deratani, A. *Macromolecules* **2010**, *43* (11), 5060–5065.
(9) Park, H.-W.; Jung, J.; Chang, T.; Matsunaga, K.; Jinnai, H. *J. Am. Chem. Soc.* **2008**, *131* (1), 46–47.
(10) Lyakhova, K. S.; Sevink, G. J. A.; Zvelindovsky, A. V.; Horvat, A.; Magerle, R. *J. Chem. Phys.* **2004**, *120* (2), 1127–1137.
(11) Schacher, F.; Yuan, J.; Schoberth, H. G.; Müller, A. H. E. *Polymer* **2010**, *51* (9), 2021–2032.
(12) Böker, A.; Reihs, K.; Wang, J.; Stadler, R.; Ober, C. K. *Macromolecules* **2000**, *33*, 1310–1320.
(13) Frenz, C.; Fuchs, A.; Schmidt, H.-W.; Theissen, U.; Haarer, D. *Macromol. Chem. Phys.* **2004**, *205*, 1246–1258.
(14) Elbs, H.; Krausch, G. *Polymer* **2004**, *45* (23), 7935–7942.
(15) Here and after the accuracy of the thickness measurements is 3 nm.
(16) Sperschneider, A.; Schacher, F.; Gawenda, M.; Tsarkova, L.; Müller, A. H. E.; Ulbricht, M.; Krausch, G.; Köhler, J. *Small* **2007**, *3* (6), 1056–1063.
(17) Sperschneider, A.; Hund, M.; Schoberth, H. G.; Schacher, F. H.; Tsarkova, L.; Müller, A. H. E.; Böker, A. *ACS Nano* **2010**, *4* (10), 5609–5616.
(18) Horvat, A.; Sevink, G. J. A.; Zvelindovsky, A. V.; Krekhov, A.; Tsarkova, L. *ACS Nano* **2008**, *2* (6), 1143–1152.